

ВОЗМОЖНОСТИ КВАНТОВЫХ ВЫЧИСЛЕНИЙ
ДЛЯ МОДЕЛИРОВАНИЯ НА ОСНОВЕ
ЭПИДЕМИОЛОГИЧЕСКИХ БОЛЬШИХ ДАННЫХ

О.Ю. Колесниченко / Olga Kolesnichenko

Институт прикладной математики имени М.В. Келдыша РАН, Москва, Россия

QUANTUM COMPUTING CAPABILITY FOR PROCESSING AND MODELING EPIDEMIOLOGICAL BIG DATA

29 May 2023

Superconducting quantum computing; **Trapped ion** quantum computer; Molecular magnet; **Nuclear magnetic resonance** quantum computer; **Neutral atoms** in optical lattices; Nonlinear optical quantum computer; Linear optical quantum computer; Quantum microprocessor based on laser photonics; Fullerene-based electron spin resonance quantum computer; Solid-state nuclear magnetic resonance Kane quantum computer; Electrons-on-helium quantum computer; **Quantum dot** computer, spin-based; Quantum dot computer, spatial-based; Cavity quantum electrodynamics; Quantum computing using engineered quantum wells; Vibrational quantum computer; Rare-earth-metal-ion-doped inorganic crystal based quantum computer; Diamond-based quantum computer; Bose-Einstein condensate-based quantum computer; Transistor-based quantum computer; Metallic-like carbon nanospheres-based quantum computer.

decoherence times

The time for which a system remains quantum-mechanically coherent

Operation times

The time it takes to perform elementary unitary transformations

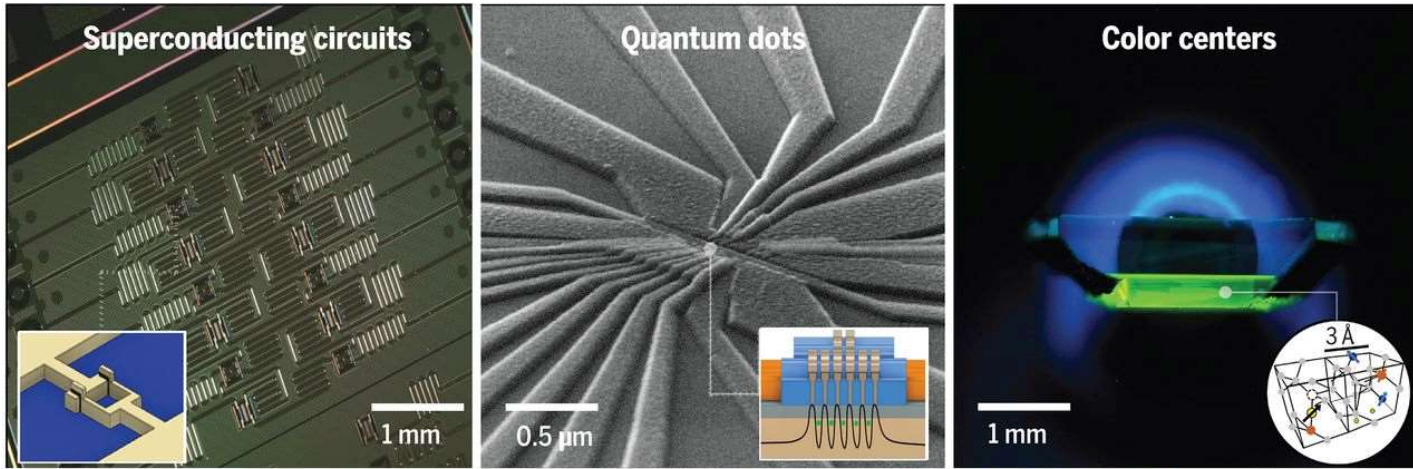
квантовая память / quantum memory
 квантовое хранилище / quantum storage
 квантовая база данных / quantum database
 quantum computing hardware
 криогенные условия ниже -200°C
 superposition, memory-memory entanglement
 (atom-photon entanglement, physically separated by 12.5 km)
 Scaling to larger systems gives rise to new materials problems.

System	τ_Q	τ_{op}	n_{op}
Nuclear spin	$10^{-2} - 10^8$	$10^{-3} - 10^{-6}$	$10^5 - 10^{14}$
Electron spin	10^{-3}	10^{-7}	10^4
Ion trap (In^+)	10^{-1}	10^{-14}	10^{13}
Electron - Au	10^{-8}	10^{-14}	10^6
Electron - GaAs	10^{-10}	10^{-13}	10^3
Quantum dot	10^{-6}	10^{-9}	10^3
Optical cavity	10^{-5}	10^{-14}	10^9
Microwave cavity	10^0	10^{-4}	10^4

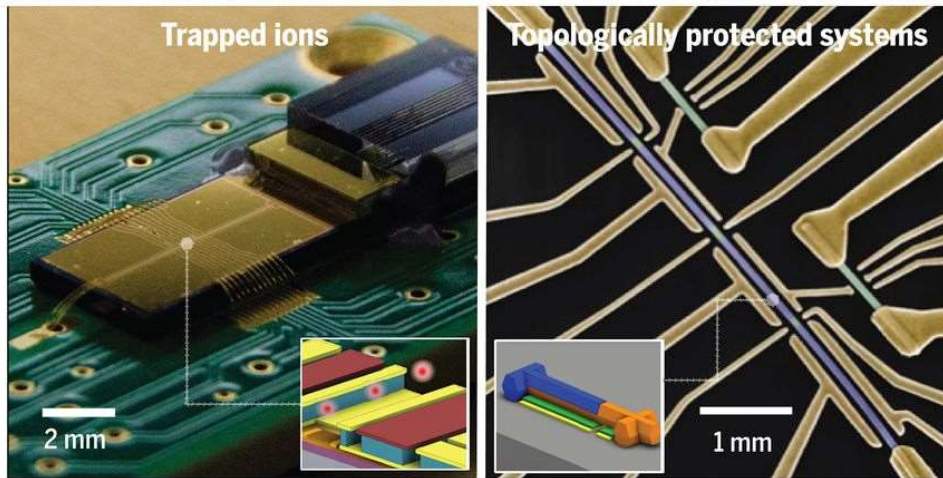
$n_{op} = \tau_Q / \tau_{op}$

Five quantum computing hardware platforms and associated sources of noise.

Platform	Where the quantum information is stored	Known sources of noise	
		Bulk materials	Surfaces and interfaces
Superconducting qubits	Energy eigenstates of Josephson junction-based electronic resonant circuits	<ul style="list-style-type: none"> • Substrate dielectric loss • Excess quasiparticles in superconducting metal cause dissipation and dephasing 	<ul style="list-style-type: none"> • Uncontrolled oxides and contaminants host two-level systems, causing dissipation and dephasing • Surface spins and charges cause flux noise and charge noise, respectively
Gate-defined quantum dots	Spin states of electrons or holes confined in electrostatic potential	<ul style="list-style-type: none"> • High mobility required for individual dot formation • Nuclear spins limit T_2 	<ul style="list-style-type: none"> • Charge traps and magnetic impurities at the dielectric interfaces • Interface inhomogeneity: Variation in valley splitting and spin-orbit coupling
Color centers	Electronic orbital and spin states	<ul style="list-style-type: none"> • Paramagnetic impurities and nuclear spins limit T_2 • Extended defects lead to strain and limit T_2^* 	Dangling bonds and electron traps at the surface affect T_2 and optical coherence for shallow NV centers
Ion traps	Electronic transitions within individual atomic ions	(Not a significant noise source)	Electric-field noise heats ion motion
Majorana zero modes	Non-Abelian topological phase of Majorana zero modes	Defect density in nanowires	Semiconductor-superconductor nanowire interface that creates a proximity hard gap



Materials challenges and opportunities
for quantum computing hardware
Nathalie P. De Leon et al.
SCIENCE 2021
Vol 372, Issue 6539
DOI: 10.1126/science.abb2823



IBM superconducting qubit processor
(Josephson junction)

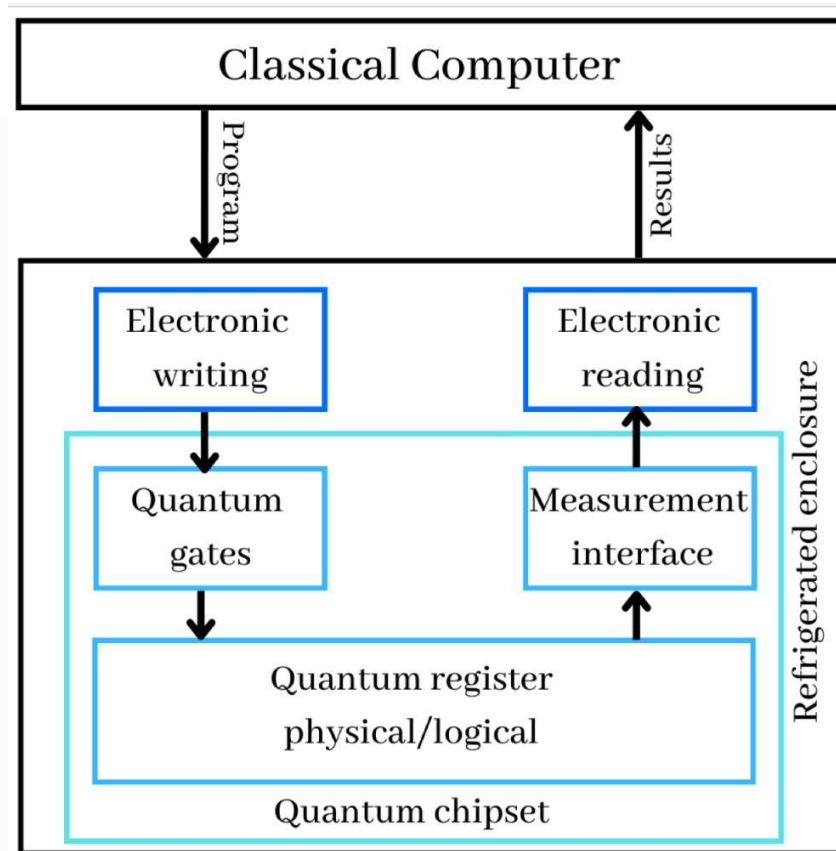
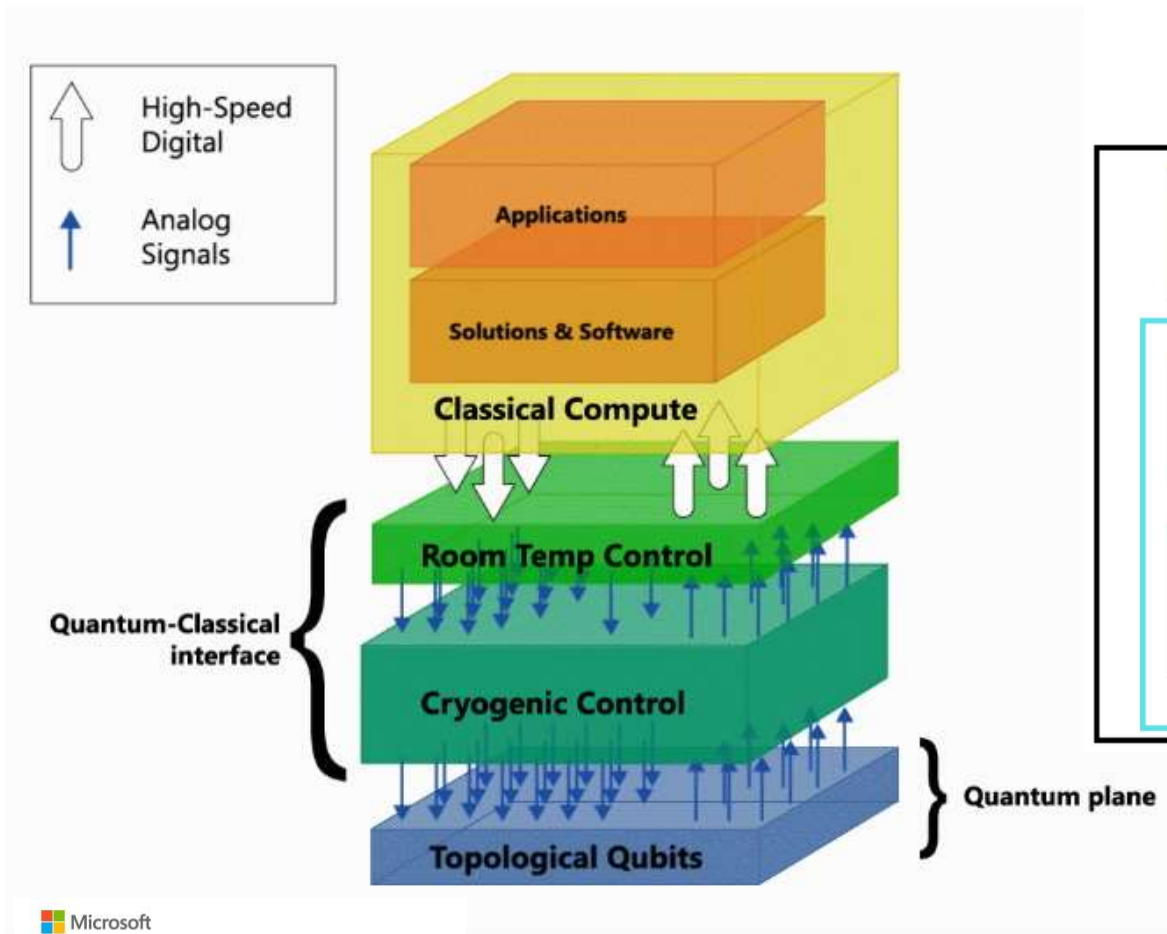
semiconductor quantum dots

color centers in diamond (atomistic model
of defects)

surface-electrode ion trap

hybrid semiconductor/superconductor,
superconducting Al /алюминий/ shell (blue)
on a faceted semiconducting InAs /арсенид
индия/ nanowire (orange)

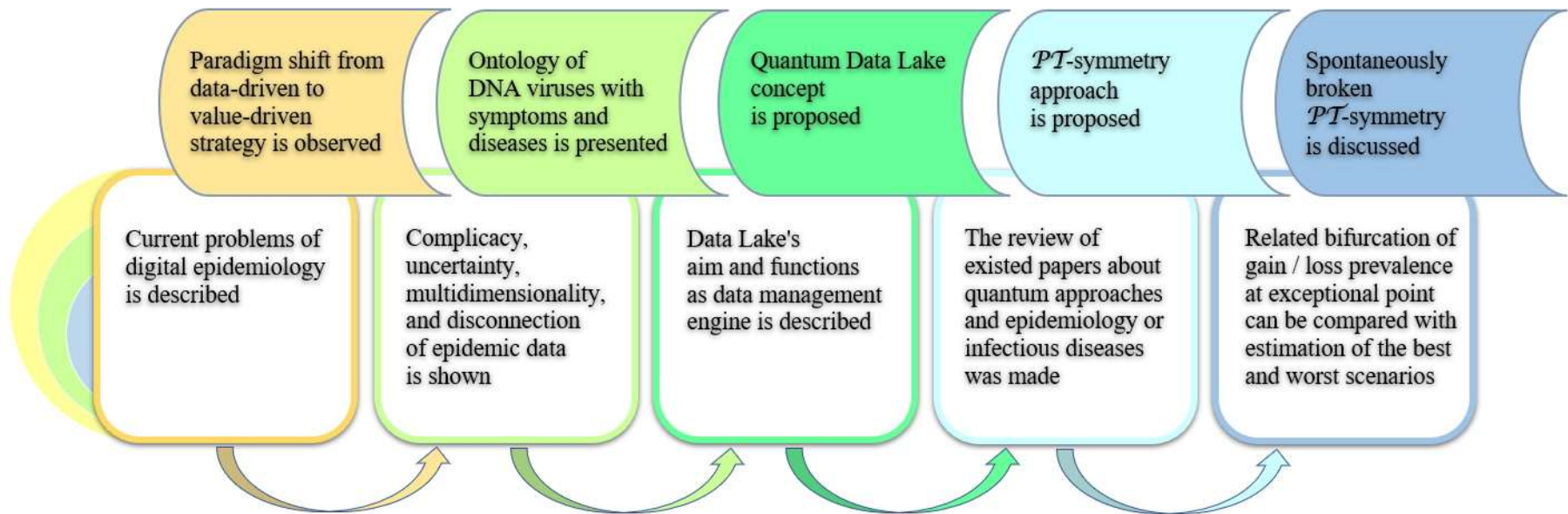
Архитектура квантового компьютера



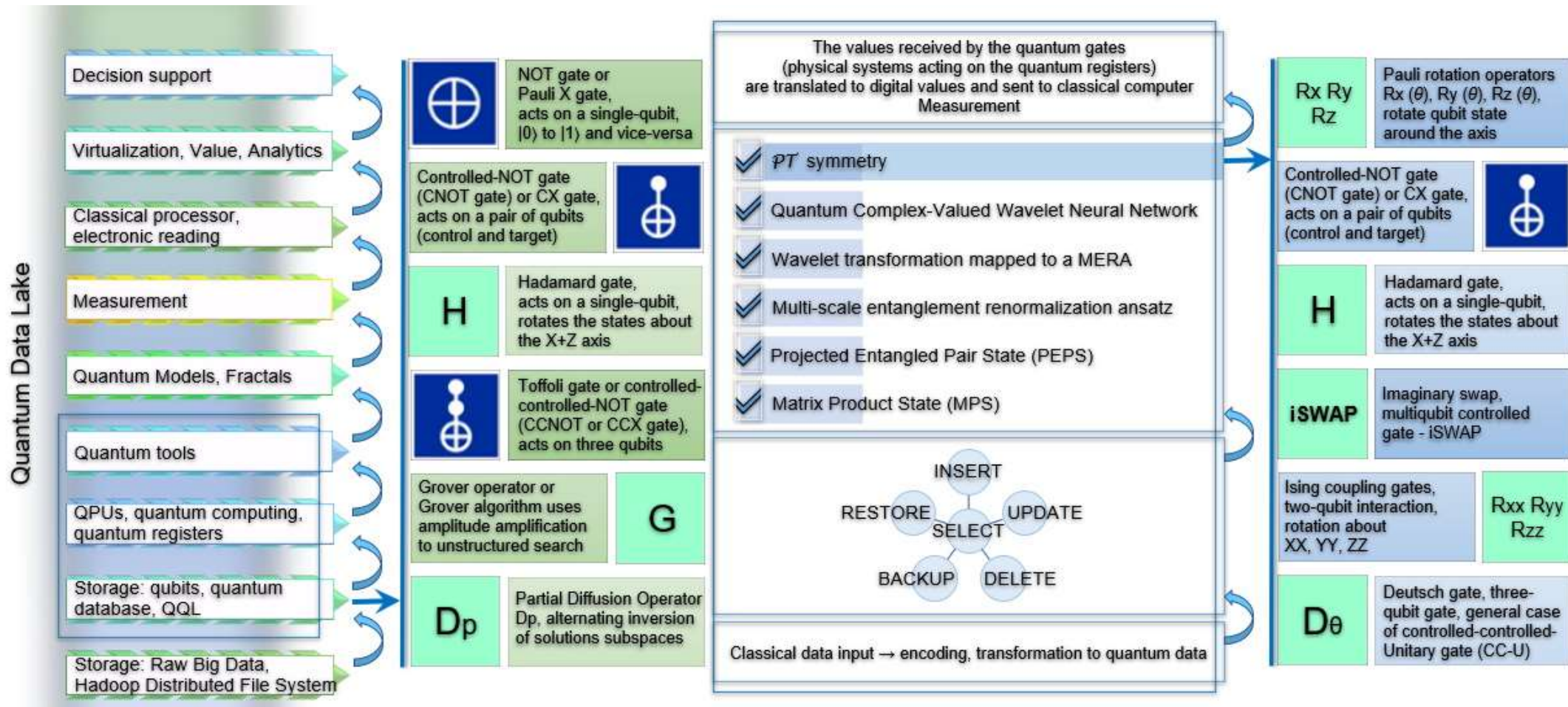
Zeguendry A., Jarir Z., Quafafou M. Quantum Machine Learning: A Review and Case Studies. Entropy. 2023; 25(2):287. <https://doi.org/10.3390/e25020287>

Microsoft

Microsoft Research Blog



Квантовое озеро данных



Фундаментальные симметрии в физике:

Charge conjugation, Parity transformation, and Time reversal symmetry

C-симметрия: смена знака заряда с частицы на античастицу

P-симметрия: одновременная инверсия (поворот) положения в пространстве трех координат

T-симметрия: теоретический обратный ход времени

Parity transformation

$$P: (x, y, z, t) \rightarrow (-x, -y, -z, t)$$

Coordinates $r(x, y, z)$

$$H(p, r, t) = H^*(-p, -r, t)$$

Time reversal

$$T: (x, y, z, t) \rightarrow (x, y, z, -t)$$

$$H(p, r, t) = H^*(-p, r, -t)$$

\mathcal{PT} -симметрия

Space-time reflection symmetry

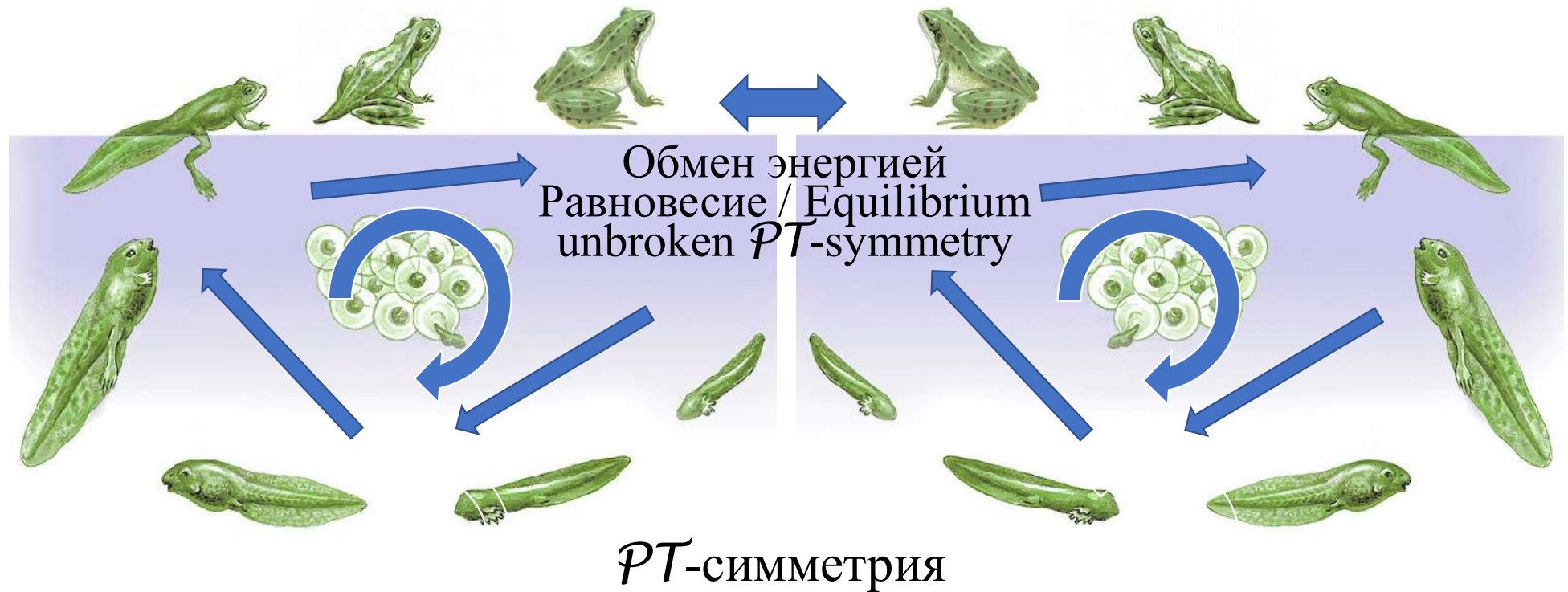
Симметрия в комплексной сфере,
одновременно отражение в пространстве и времени.
Впервые описана Bender С.М. и Boettcher S. в 1998 году.

Square-root singularities или

exceptional point (Bender-Wu singularities) in the complex- g plane, где
 g – константа, связывающая два энергетических состояния Гамильтониана:
состояние a и состояние b (энергия не дискретна).

$$H \text{ (оператор полной энергии системы)} = \begin{pmatrix} a & g \\ g & b \end{pmatrix}$$

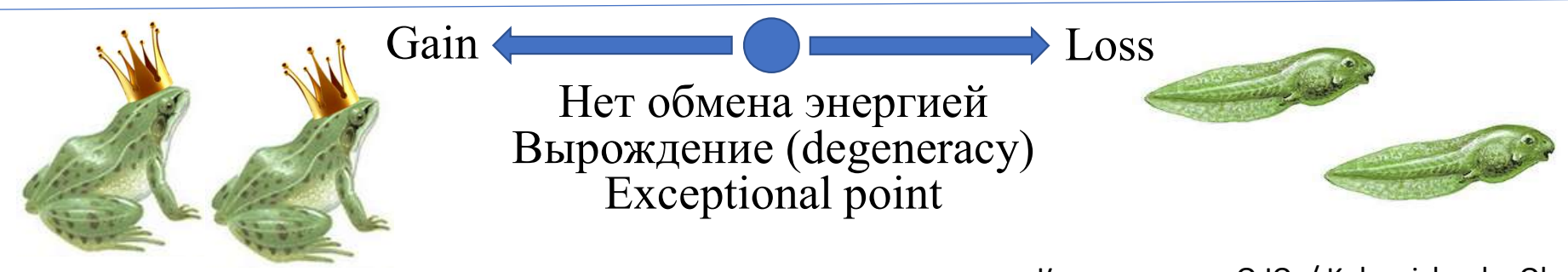
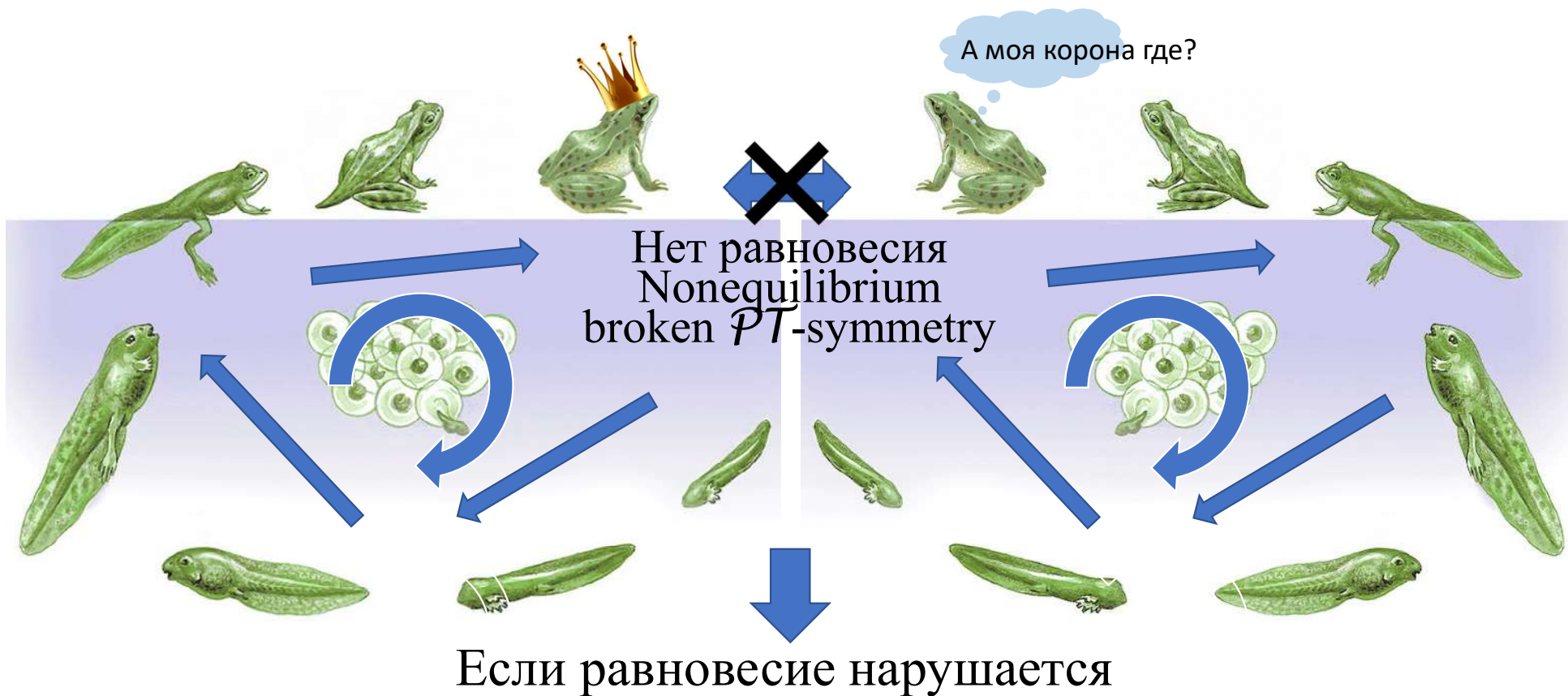
$$H(p, r, t) = H^*(p, -r, -t)$$



Parity transformation – зеркальное отражение.

Time reversal – обратный ход времени в развитии (эволюции) системы.

Одновременное зеркальное отражение и обратный ход времени при неизменности всех частей системы соответствует **симметрии**.





Carl Bender

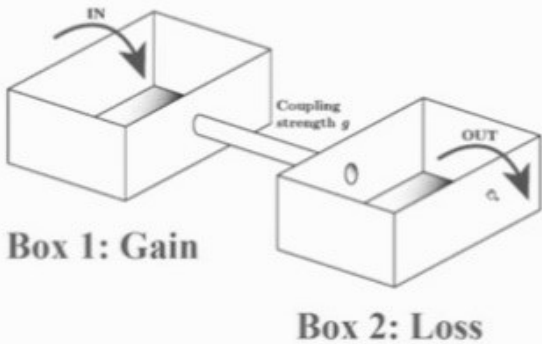
Theoretical Physics Colloquium

Parity-Time (PT) Symmetry



Theoretical-Physics-Colloquium

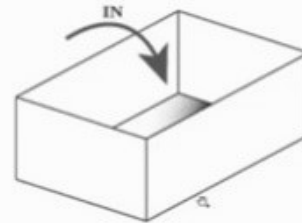
Couple the boxes



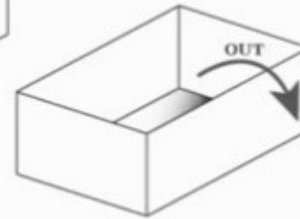
$$H_{\text{coupled}} = \begin{bmatrix} a + ib & g \\ g & a - ib \end{bmatrix}$$

This Hamiltonian is not Hermitian but it is *PT* symmetric

Two noninteracting closed boxes, one with gain, the other with loss:



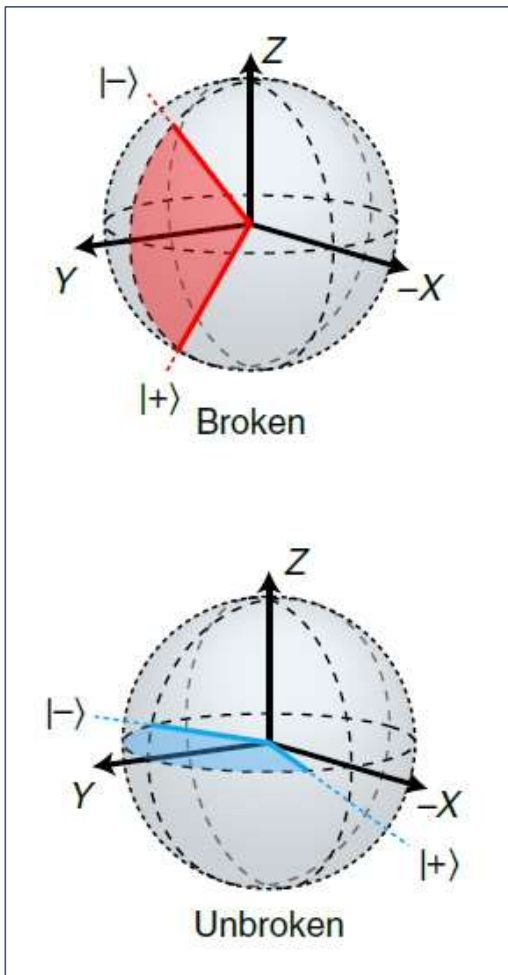
Box 1: Gain



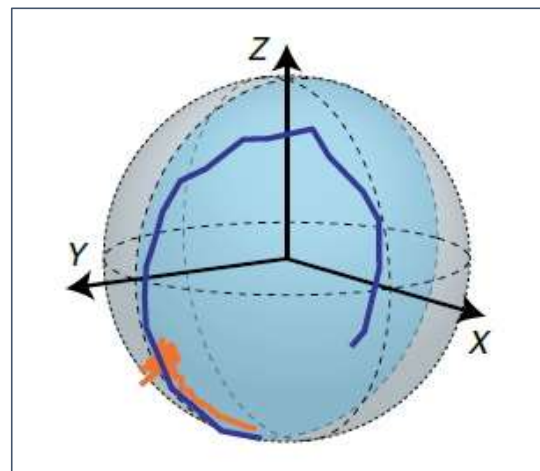
Box 2: Loss

$$H_{\text{combined}} = \begin{bmatrix} a + ib & 0 \\ 0 & a - ib \end{bmatrix}$$

This system is *not in equilibrium*



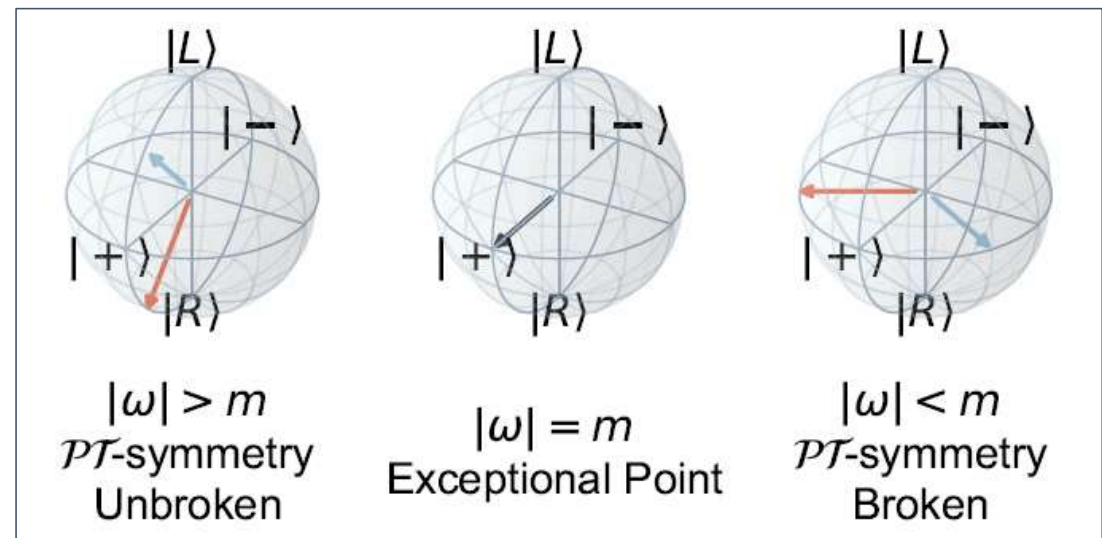
Non-orthogonality of eigenstates in the vicinity of the EP. The eigenstates in the broken (unbroken) region lie in the Y-Z (X-Y) plane (Bloch spheres). The calculated angles for the eigenstates in the broken (a) and unbroken (b) regions.



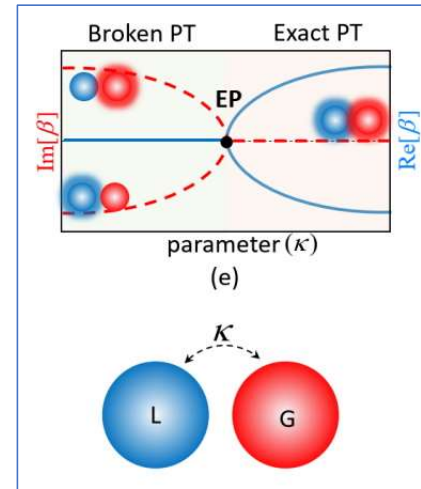
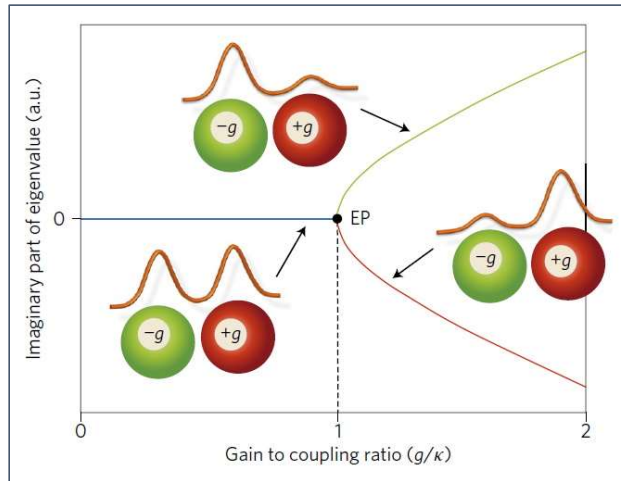
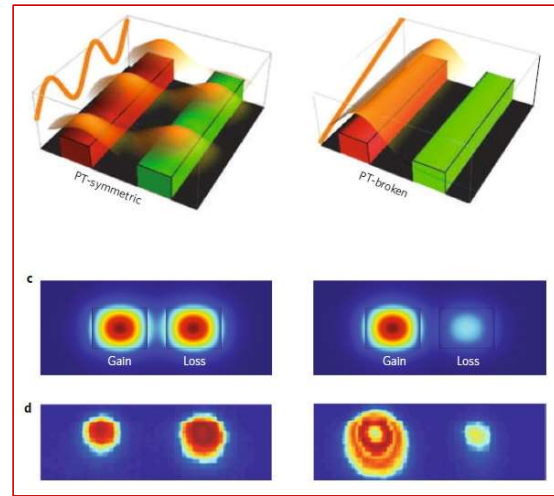
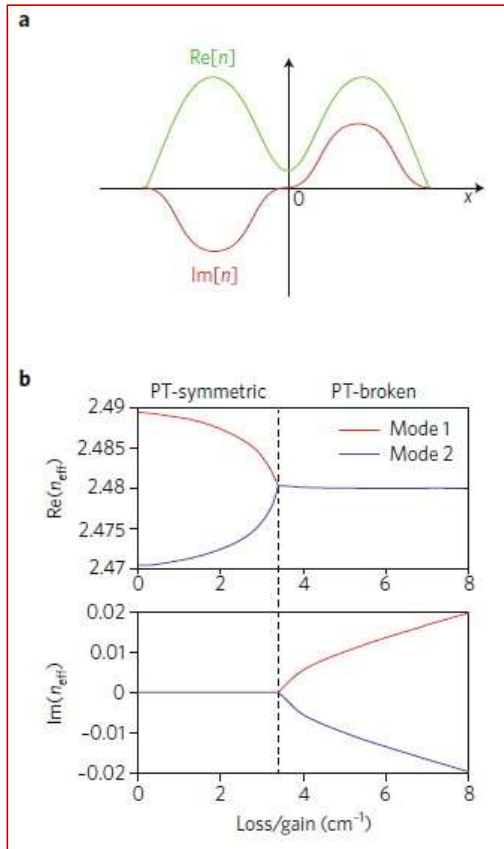
Evolution of the quantum state in the Bloch sphere for parameters in the PT-broken region (orange) and in the PT-symmetric region (blue).

The arrows represent the eigenvectors. PT-symmetry is unbroken. The eigenmomenta are a pair of real numbers with opposite signs. At the exceptional point the eigenmomenta are coalescing to 0. PT-symmetry is broken. The eigenmomenta are a pair of purely imaginary numbers with opposite signs.

Naghiloo, M.; Abbasi, M.; Joglekar, Y.N.; Murch, K.W. Quantum state tomography across the exceptional point in a single dissipative qubit. *Nature Physics* 2019, 15, 1232–1236. <https://doi.org/10.1038/s41567-019-0652-z>



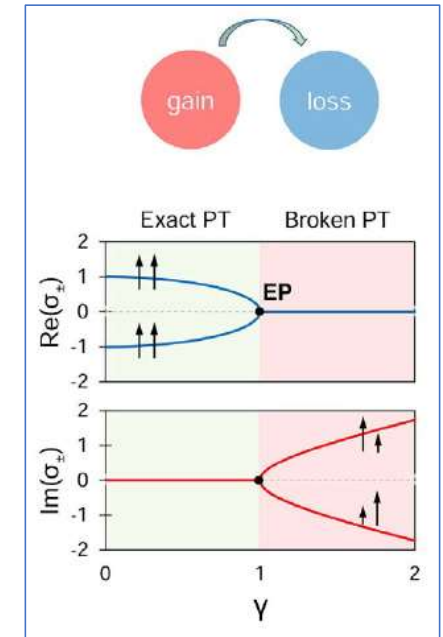
Song, X.; Murch, K. Parity-time symmetric holographic principle. Preprint arXiv 2022, 2210.01128v1. <https://doi.org/10.48550/arXiv.2210.01128>



System of two coupled waveguides. Schematic transition in the eigenvalues from purely real (exact PT symmetry) to purely imaginary (broken PT symmetry) in an active balanced system.

Krasnok, A.; Nefedkin, N.; Alú, A. Parity-Time Symmetry and Exceptional points: A Tutorial. Preprint arXiv 2021, 2103.08135v1. <https://doi.org/10.48550/arXiv.2103.08135>

El-Ganainy, R.; Makris, K.G.; Khajavikhan, M.; Musslimani, Z.H.; Rotter, S.; Christodoulides D.N. Non-Hermitian physics and PT symmetry. *Nature Physics* 2018, 14, 11–19. <https://doi.org/10.1038/nphys4323>



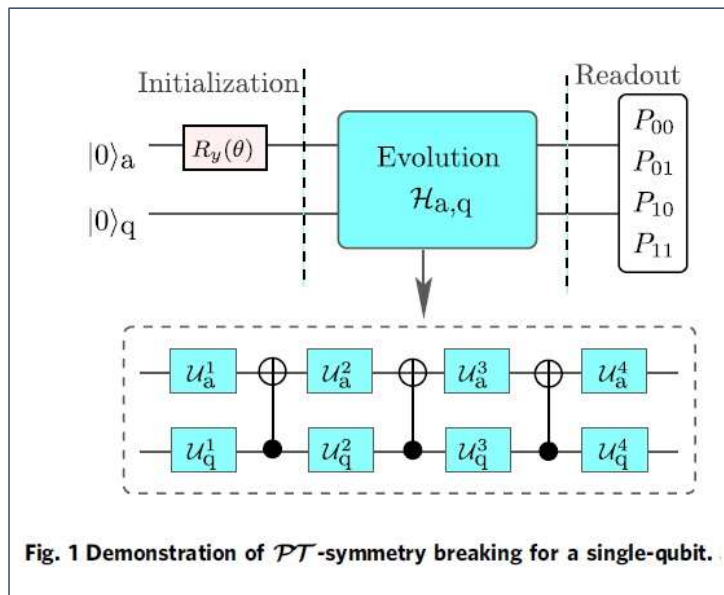
PT-symmetric system of two coupled waveguides (top) with gain (red) and loss (blue), and the corresponding eigenvalues (bottom) versus the gain-loss contrast. Transition in the eigenvalues from purely real (exact PT symmetry) to purely imaginary (broken PT symmetry).

Miri, M.-A.; Alú, A. Exceptional points in optics and photonics. *Science* 2019, 363 (6422). <https://doi.org/10.1126/science.aa17709>

PT symmetry and phase transition in photonics. Schematics of the optical potential and its realization using two coupled waveguides.

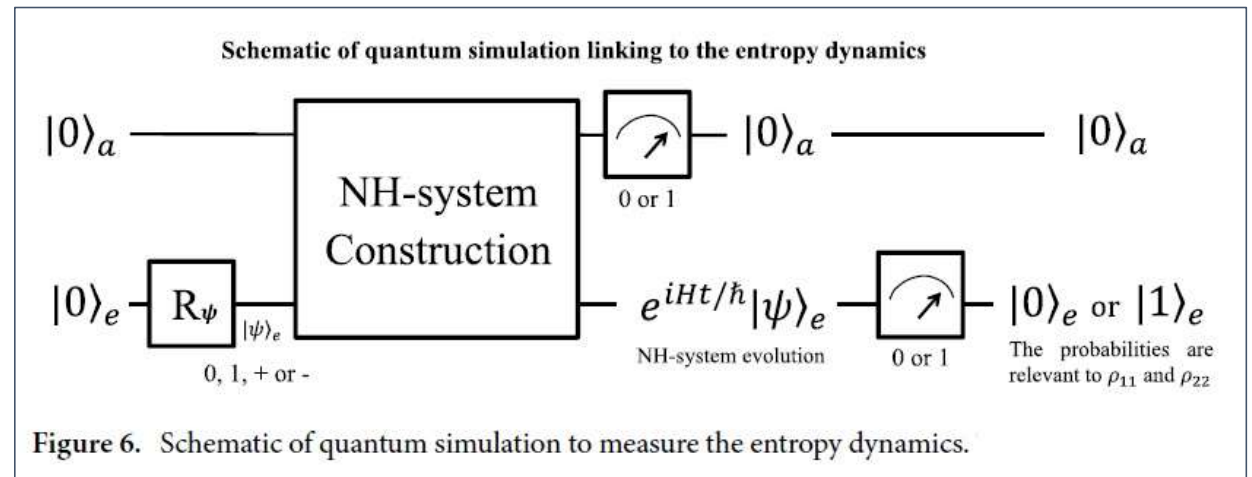
Feng, L.; El-Ganainy, R.; Ge, L. Non-Hermitian photonics based on parity-time symmetry. *Nature Photonics* 2017, 11, 752–762. <https://doi.org/10.1038/s41566-017-0031-1>

PT exact phase. The two eigenmodes are distributed over both sites and neither of them experiences a net gain or loss that is, they remain neutral.
PT-broken phase. The symmetry of each mode is broken such that one of them resides mostly in the gain cavity (and hence enjoys amplification) while the other one inhabits the lossy resonator (experiences attenuation).

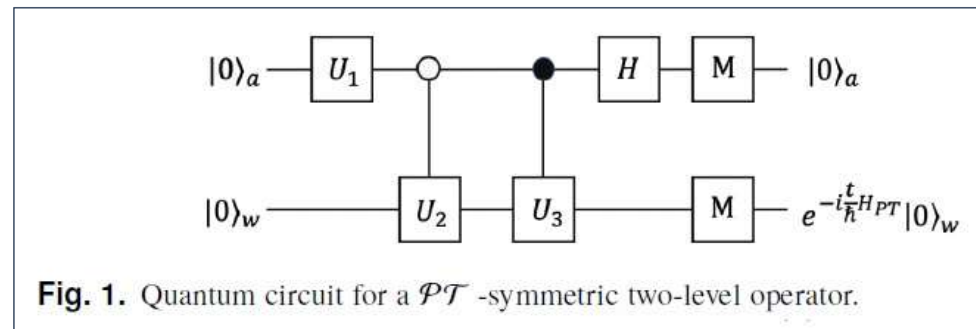


Dogra, S.; Melnikov, A.A.; Paroanu, G.S. Quantum simulation of parity–time symmetry breaking with a superconducting quantum processor. *Communications Physics* 2021, 4, 26. <https://doi.org/10.1038/s42005-021-00534-2>

Gao, W.-C.; Zheng, C.; Liu, L.; Wang, T.-J.; Wang, C. Experimental simulation of the parity-time symmetric dynamics using photonic qubits. *Optics Express* 2021, 29 (1), 517–526. <https://doi.org/10.1364/OE.405815>



Zheng, C.; Li, D. Distinguish between typical non-Hermitian quantum systems by entropy dynamics. *Scientific Reports* 2022, 12, 2824. <https://doi.org/10.1038/s41598-022-06808-1>



Zheng, C.; Hao, L.; Long G.L. Observation of a fast evolution in a parity-time-symmetric system. *Philosophical Transactions of the Royal Society A: Mathematical, Physical and Engineering Sciences* 2013, 371 (1989), 20120053. <https://doi.org/10.1098/rsta.2012.0053>

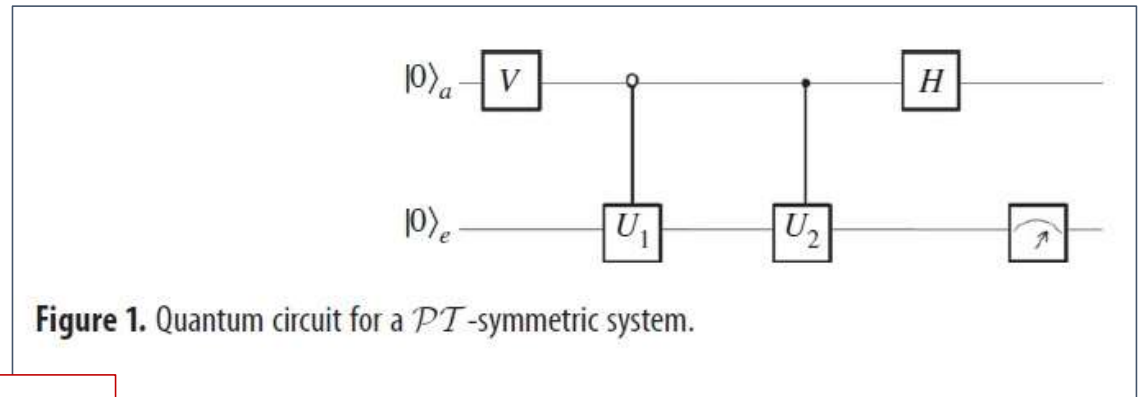


Figure 1. Quantum circuit for a \mathcal{PT} -symmetric system.

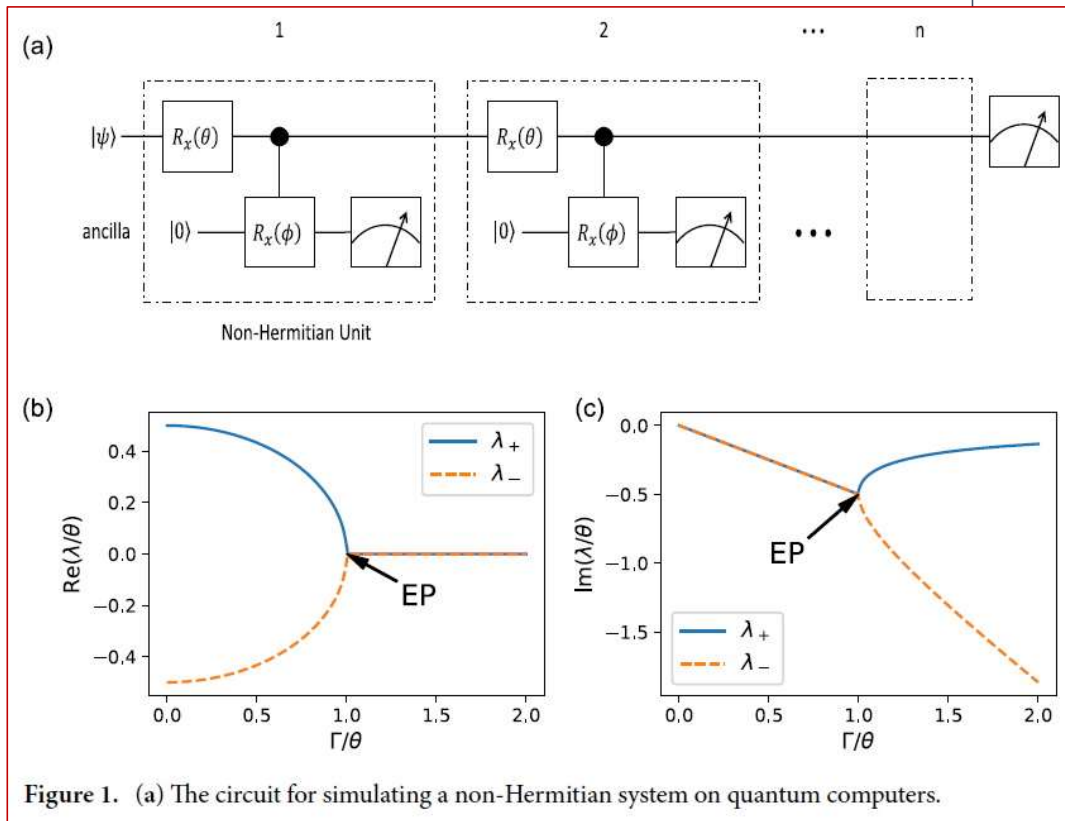


Figure 1. (a) The circuit for simulating a non-Hermitian system on quantum computers.

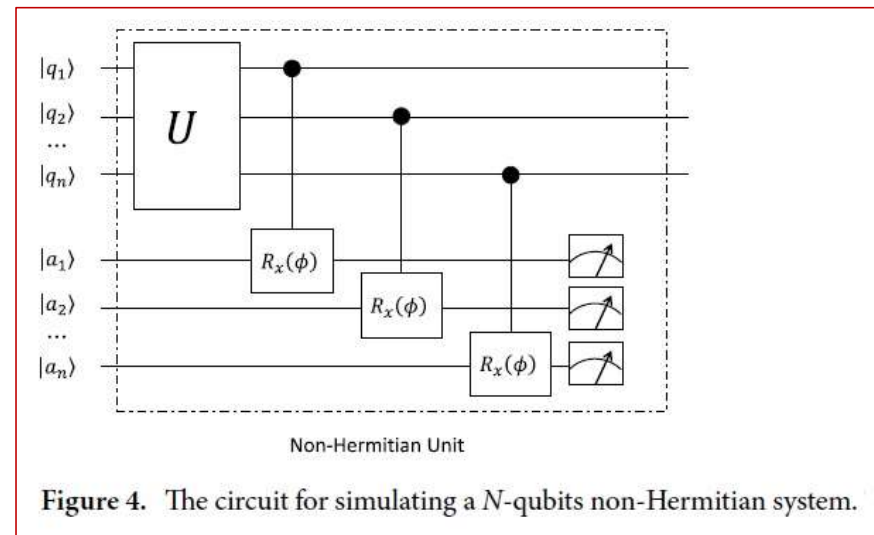
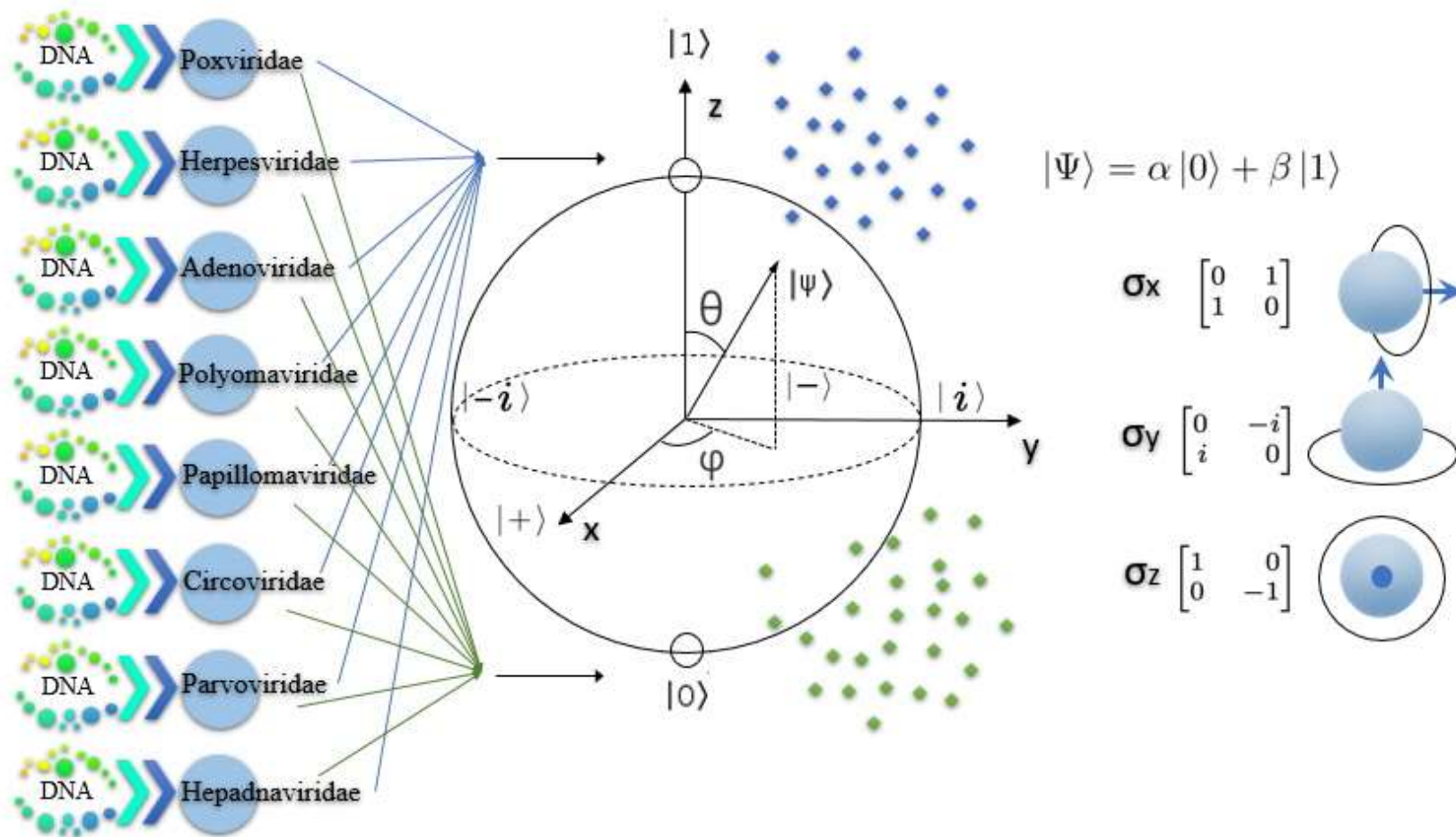


Figure 4. The circuit for simulating a N -qubits non-Hermitian system.

Zhang, G.-L.; Liu, D.; Yung, M.-H. Observation of exceptional point in a \mathcal{PT} broken non-Hermitian system simulated using a quantum circuit. *Scientific Reports* 2021, 11, 13795. <https://doi.org/10.1038/s41598-021-93192-x>



Данные в эпидемиологии

Dynamics over time



Climate / ecological data



Virus carriers in nature data



Global / local mobility data



Social data



Transmission data



Vaccination data



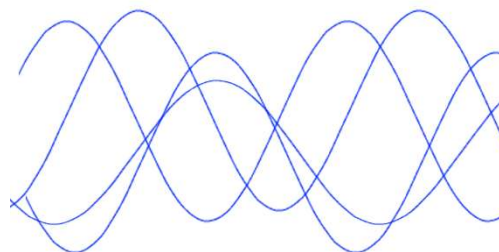
Electronic health records data



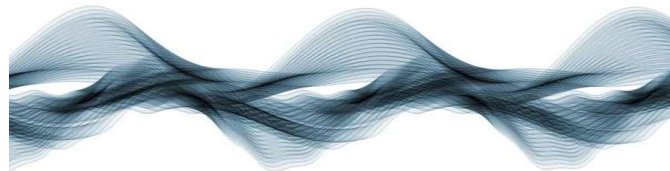
Human Omics data



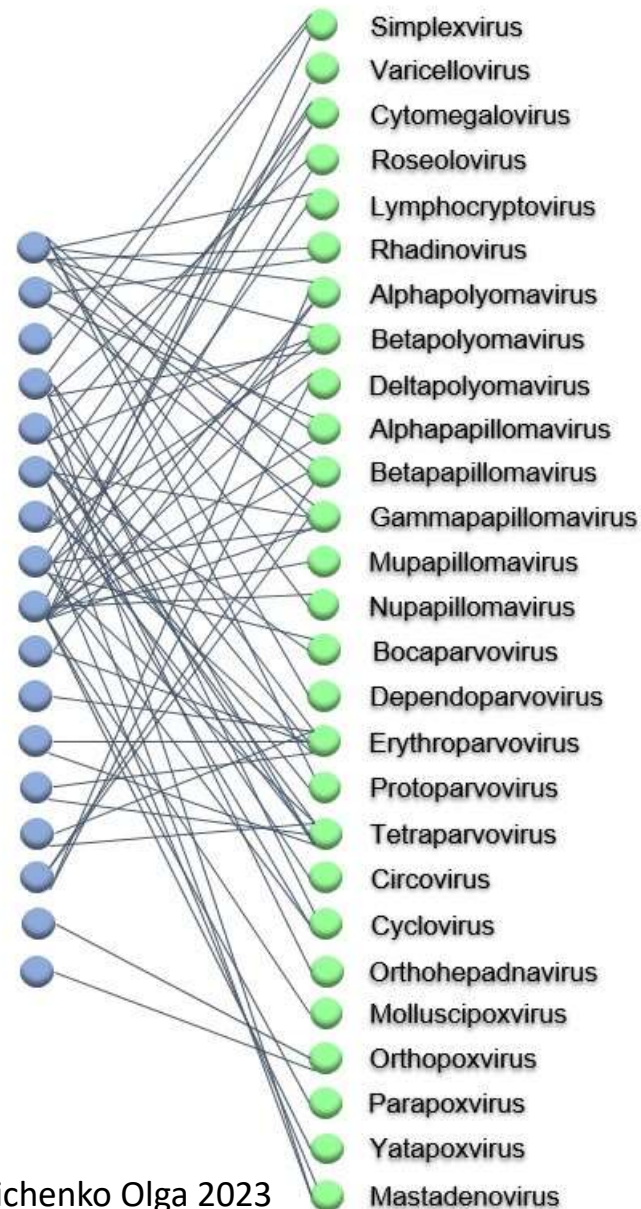
Virus Omics data

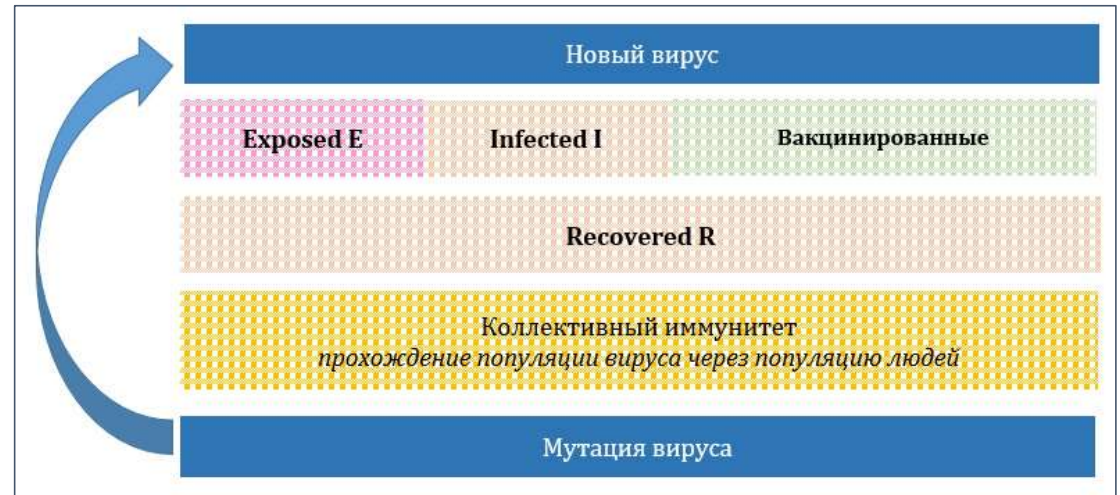
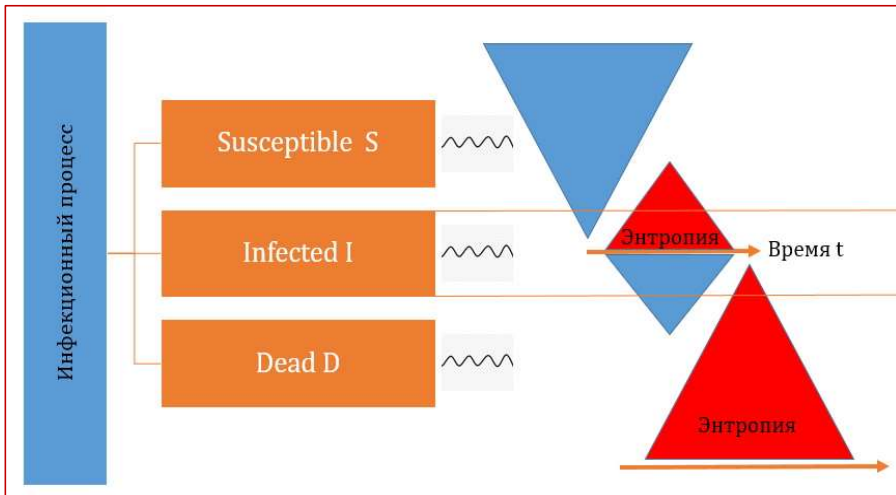
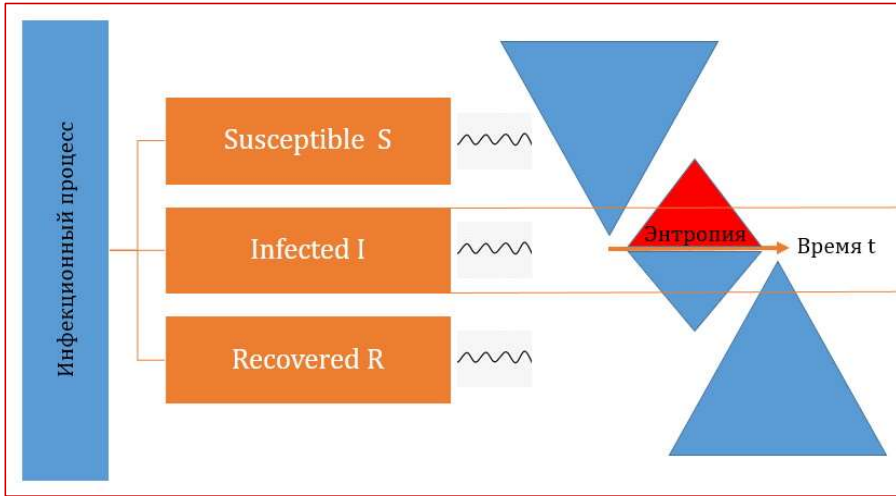


Наращение энтропии
и “обратный ход времени”

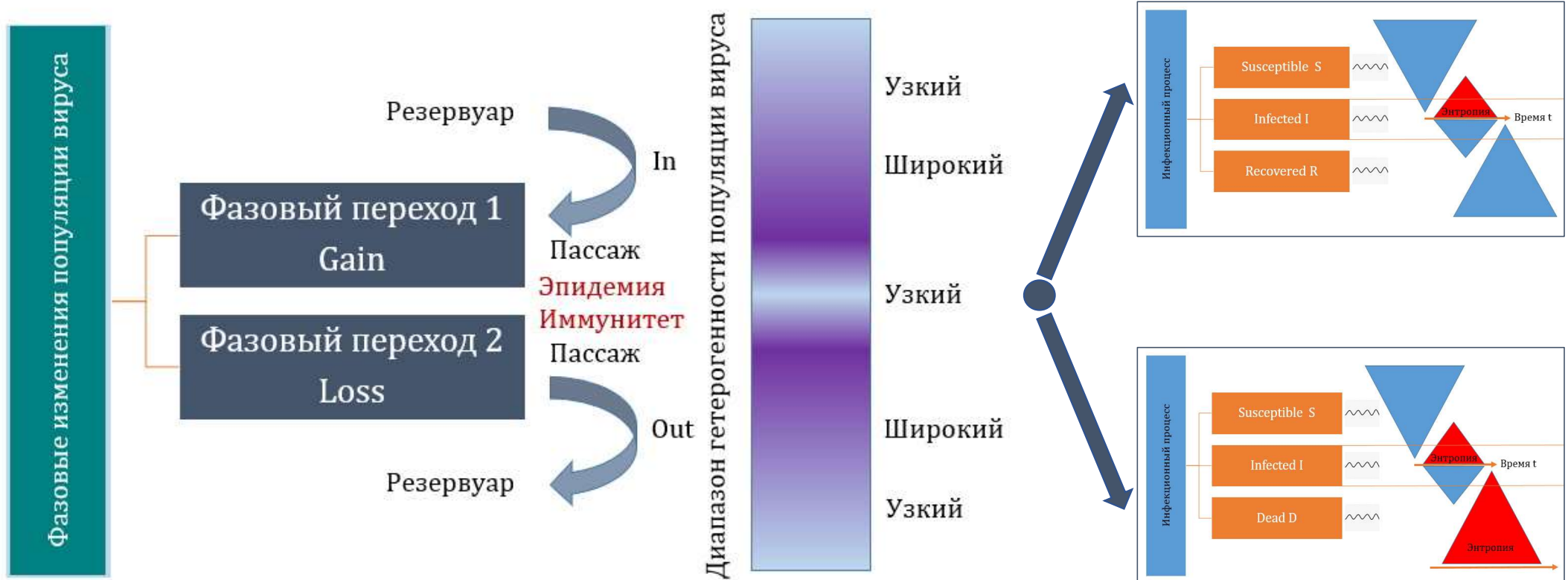


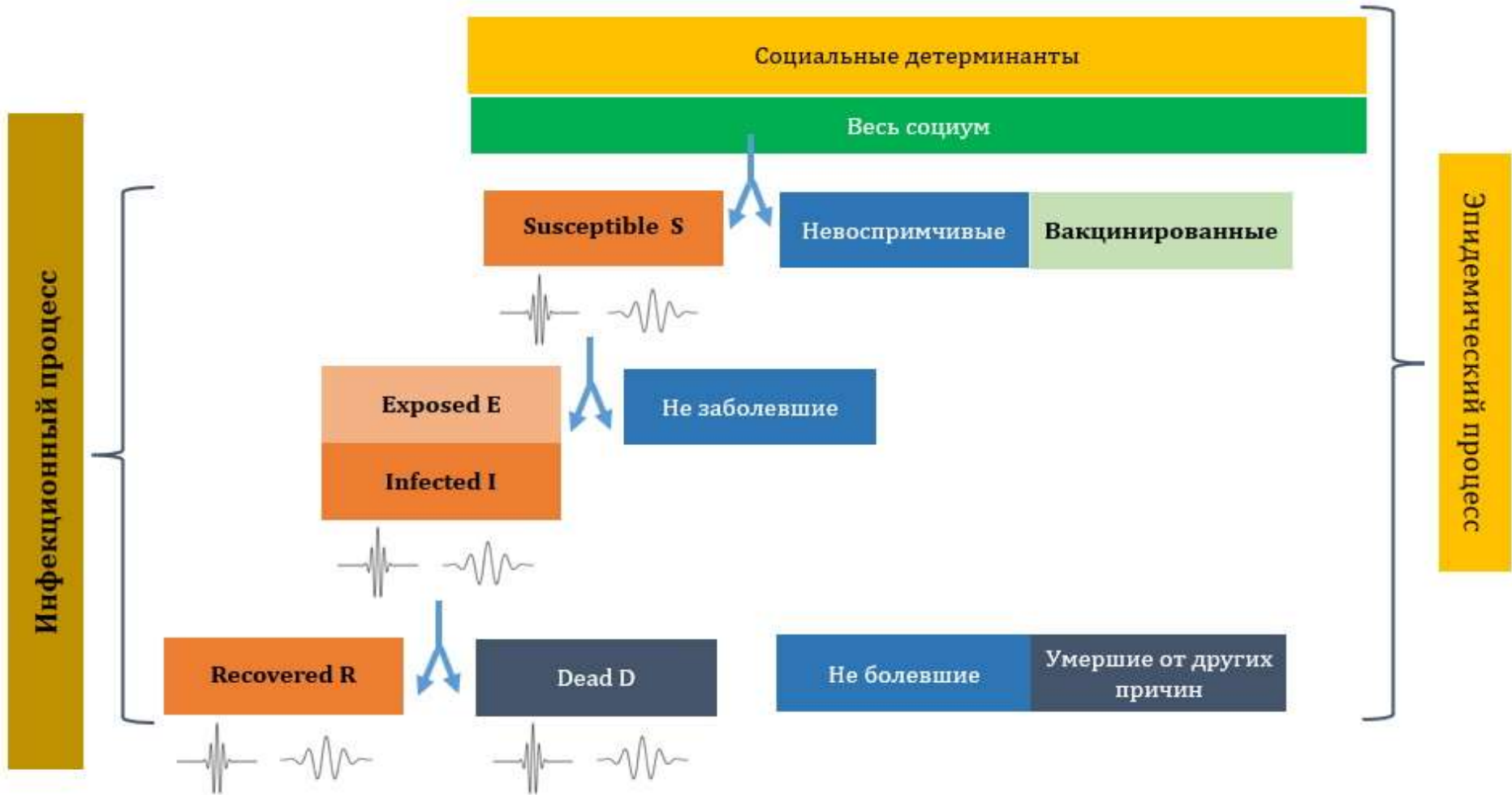
cancer
benign tumors
genital infections
meningitis, encephalitis
hepatitis
gastroenteritis
nephritis
respiratory diseases
skin lesions
vasculitis
myocarditis, pericarditis
arthritis
anaemia
fetal damage and loss
asymptomatic presence
monkeypox
smallpox

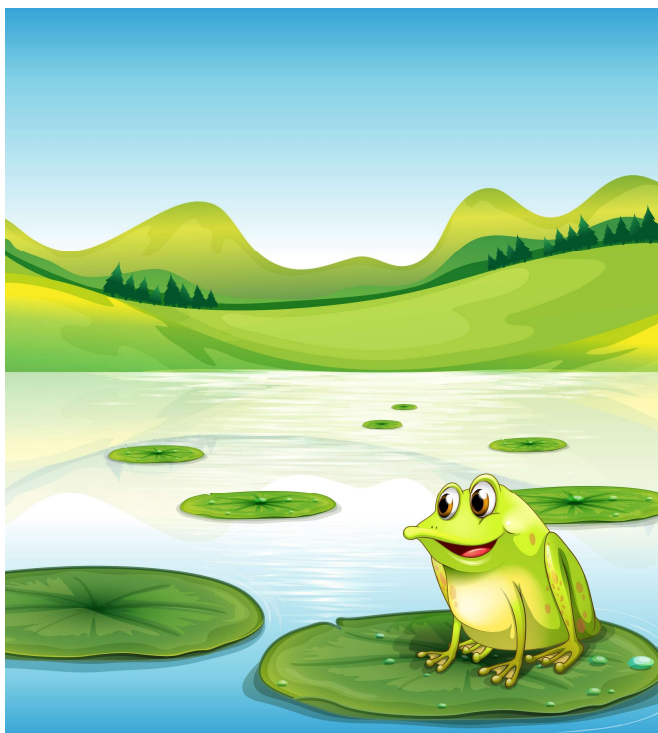




В.Д. Беляков, “Общие закономерности функционирования паразитарных систем (механизмы саморегуляции)”, Паразитология, Т. XX, № 4, С. 246–255, 1986.







Спасибо за внимание!
oukolesnichenko@list.ru